ISSN:1813-1786 (Print) 2313-7770 (Online)

Comparing Von-Mises Stress in Various Geometrical Configurations of a Rectangular Plate with a Central Hole

M. S. Ali[1], S. K. Chatha[2], Z. Ahmed[3]

[1,2,3] *Mechanical Engineering Department, University of Engineering and Technology, Lahore, Pakistan.*

[1]sherali0514@gmail.com

Abstract- The finite element method (FEM) is widely used in structural analysis, but complex geometries and boundary conditions can result in high computational costs. To address this concern, this study investigates the use of symmetry-based simplification in finite element analysis of a rectangular plate with a central circular hole subjected to uniaxial tensile loading. The novelty of this research lies in quantitatively comparing the von Mises stress results of four geometrical configurations: full plate, left half plate, lower half plate and quarter plate. Simulations were performed using the Abaqus under plane stress conditions, and results were validated against analytical solutions derived from the Kirch's equations. The comparison showed that all models produced von Mises stress results with a maximum deviation of less than 5% from the analytical values. Notably, the quarter plate model yielded reliable results while significantly reducing computational time and resources, making it an optimal choice for symmetric structures.

Keywords- Finite Element Analysis, Abaqus, Plate, Axes of Symmetry, Von-Mises Stress.

I. INTRODUCTION

A plate is a two-dimensional structural member that has two of its dimensions significantly larger than the third one. It can be considered as a two-dimensional variant of a beam which is often dealt with as a one-dimensional structural member. Plates are categorised into thin and thick plates. If the smallest dimension, also referred to as the thickness of the plate, is between 0.01 and 0.1 of its larger dimensions then it is called a thin plate and if the thickness is larger than 0.1 of the larger dimensions than the plate is referred as a thick plate. Plates might be used to bear loads applied perpendicular to their surface or axial loads applied along the surface. These axial loads can be tensile or compressive in nature. Moreover, the nature of the load may also vary depending upon the directions that it is applied in. A load applied in one direction only is termed as a uniaxial load while a load being applied in two directions along the surface of the plate is usually called a biaxial load.

The plane stress condition is an appropriate approximation when dealing with plate problems that have uniaxial or biaxial surface loads applied on them and there is no loading in the perpendicular direction. The condition of plane stress simplifies the overall stresses by ignoring the normal stress and the shear stresses along the perpendicular direction of the plate surface. In other words, instead of dealing with nine stress components σ_x, σ_y, σ_z, τ_{xy}, τ_{yx},τ_{yz},τ_{zy},τ_{xz} and τ_{zx}, we only have to deal with three stress components namely, σ_x, σ_y, andτ_{xy}.

It is often useful to calculate the maximum and minimum normal stresses and maximum and minimum shear stresses. These stresses are also referred to as the principal stresses. These principal stresses act along particular angles from the normal direction. These principal stresses are related to the normal stresses σ_x and σ_y, and the shear stress τ_{xy}.

$$\sigma_1, \sigma_2 = \frac{\sigma_x + \sigma_y}{2} \pm \sqrt{\left(\frac{\sigma_x - \sigma_y}{2}\right)^2 + {\tau_{xy}}^2} \qquad (1)$$

The von Mises stress is an equivalent stress value which is used to predict failure according to the distortion energy theory for members subjected to static loading. According to the Distortion Energy theory, a particular material subjected to any type of static load yields when its distortion strain energy per unit volume becomes equal to the distortion strain energy per unit volume of the material when it is subjected to simple tension or compression. The total strain energy can be expressed as a sum of hydrostatic strain energy which corresponds to the change in volume and the distortion strain energy which corresponds to the change in shape.

$$U = U_h + U_d \qquad (2)$$

By calculating the total strain energy and the hydrostatic strain energy, we can obtain an

expression for the distortion strain energy in terms of the principal stresses, Young's modulus and the Poisson's ratio. Once we have the distortion strain energy, it can be equated to the distortion strain energy of the material under simple tensile loading as it fails. This results in the expression of von Mises stress:

$$\sigma_v = \sqrt{\sigma_1{}^2 + \sigma_2{}^2 + \sigma_3{}^2 - \sigma_1\sigma_2 - \sigma_2\sigma_3 - \sigma_1\sigma_3} \quad (3)$$

For plane stresses this simplifies to:

$$\sigma_v = \sqrt{\sigma_1{}^2 + \sigma_2{}^2 - \sigma_1\sigma_2} \quad (4)$$

This value of von Mises stress is very convenient as it can simply be compared with the yield strength of the material to predict if it will fail or not [1]. By substituting the values of the plane stresses from Eq. (1) into Eq. (4), it can be shown that:

$$\sigma_v = \sqrt{\sigma_x{}^2 + \sigma_y{}^2 - \sigma_x\sigma_y + 3\tau_{xy}{}^2} \quad (5)$$

When using stress equations, it is assumed that the structural members do not contain any geometric discontinuities and are uniform along all dimensions. However, in the real world it is simply not possible to attain a perfectly uniform structural member. Moreover, often machine components require certain changes or discontinuities in their structures for the purpose of using fasteners such as bolts. In a similar manner, shafts require changes in their diameter along their length to accommodate bearings. Such discontinuities end up disrupting the usual stress distributions and create areas of stress concentrations at the locations where the geometry change takes place [2-3]. These sudden geometric changes are often referred as stress raisers. It is not quite easy to tackle with such cases theoretically therefore we define a stress concentration factor K_t to relate the actual maximum stress with the calculated stress [4].

$$K_t = \frac{\sigma_{max}}{\sigma_{calculated}} \quad (6)$$

The values for the stress concentration factor vary depending on the type of element that it is used on [5], the change in geometry and the nature of the load. These values are found out by conducting a large number of experiments and then applying curve-fitting technique on the data. The usual practice in engineering is to use the charts or graphs constructed by using these curves.

The finite element analysis proves to be very useful when determining if a part will fail under the given loads and boundary condition [6].

It can be used to discretise a larger structural member into small elements to calculate von Mises stresses at all the nodes of these elements. This can be easily accomplished for relatively simple geometries under simple loading conditions but when dealing with complex structural problems, it becomes essential to simplify the problem to reduce the computation time and work within the computational limits of the machine [7]. One way to achieve this is simplify three-dimensional problems into two-dimensions by using plane stress or plane strain conditions. Another method which can be utilised involves simplifying the geometry by reducing its size according to the axes of symmetry it possesses. Generally, for each axis of symmetry the size of the model can be reduced to half [8]. However, to take advantage of this it must be understood what qualifies as an axis of symmetry. Along with the geometrical shape, the applied loads and the boundary conditions must also be same on the both sides of the axis of symmetry [9].

In modern engineering design, it is essential to balance the fidelity of finite element simulations with the constraints of computational resources. When analyzing structural elements such as plates with discontinuities like holes, it becomes crucial to simplify the model without compromising accuracy. This study addresses the problem of whether symmetry-based reductions in model geometry can reliably predict stress distributions particularly von Mises stress when compared to a full-model analysis and analytical solutions.

This research work focuses on evaluating the effectiveness of symmetry-based simplification in finite element analysis of a rectangular plate with a central hole under uniaxial loading. The primary objectives of this work are to assess the impact of geometric simplification along symmetry axes on the accuracy of von Mises stress calculations. To compare various symmetric configurations with the full model against analytical results. To determine the optimal balance between computational efficiency and accuracy in stress prediction. The novelty of this study lies in its comparative approach to evaluating stress predictions across different symmetrical reductions of a plate with a central discontinuity. While symmetry is widely known and utilized in FEA, this work quantitatively benchmarks the trade-off between computational efficiency and accuracy using both numerical and analytical methods, which is crucial in modern design and optimization workflows [10].

II. METHODOLOGY

A. Method Description

A thin plate with a hole at the centre, subjected to uniaxial tensile load, was considered for this analysis. The plate was assumed to have constant cross-section and complete homogeneity in its material properties. This three-dimensional problem was dealt with as a two-dimensional problem by making use of the plane stress conditions. The

dimensions along with the magnitude of loads and the material properties of the plate are presented in the table below.

Table-I: Dimensions, Loads and Material Properties of the Plate

Parameter	Description
Young's Modulus (MPa)	70000
Poisson's Ratio	0.33
Length (mm)	140
Diameter of Hole (mm)	20
Width (mm)	70
Thickness (mm)	5
Uni-axial Tensile Distributed Load (MPa)	50

B. Modelling

A total number of four models of the plate described above were created in Abaqus [11]. The modelling of all models involved the same steps except in the sketching part. The details of these models are presented below:

Table-II Details of Different Models used for Analysis

Name	Size Reduction Factor	Partitions	Axes of Symmetry
Full Plate	1	4	2
Left Half Plate	0.5	2	1
Lower Half Plate	0.5	2	1
Quarter Plate	0.25	0	0

All models of the plate were modelled as two-dimensional deformable shells with the dimensions specified above. The models possessing one or two axes of symmetry were split into partitions along those axes to aid in symmetric meshing [12]. The material of the plate was modelled as an elastic and isotropic material with specifications already discussed. A solid and homogeneous section with thickness of 5 mm was assigned to the plate models to aid in the calculations when using the plane stress model.

C. Meshing

Non-uniform meshing was chosen to suit the nature of the method as the stresses towards the centre were predicted to be high and of more importance. The outer edges of the models were seeded with elements of size 5mm while the edge of the hole was assigned an element size of 1mm. The axes of symmetry were meshed using single bias with the element size decreasing from 5mm to 1mm from the outer edges to the edge of the hole. The element shape was chosen to be quadrilateral and structured meshing was used [13]. The geometric order of the shape function was chosen to be linear and plane stress elements were used.

D. Application of Loads and Boundary Conditions

All finished parts were used to create instances in their respective assemblies. Steps were created for all the models to apply the loads. For the full plate model, a pressure load of magnitude -50 (minus sign to signify tensile load) was applied on both the left and right sides. For the model of the left half plate, the pressure load was only applied to the left side and on the right side a symmetry boundary condition was applied with symmetry in x direction (XSYMM) turned on. For the lower half plate model, pressure loads of magnitude -50 were applied on both sides and a symmetry boundary condition was used with symmetry in y direction (YSYMM) turned on. Finally for the quarter plate, the pressure load of -50 was applied on the left side only. Two symmetry boundary conditions were utilised in this case on the right side and the top side of the model. The one on the right was set at symmetry in x direction (XSYMM) while the one on the top edge was set at symmetry in y direction (YSYMM).

E. Analysis

Jobs were created for all the models to generate output databases. For each model, three paths were created. The first path was created from the left edge to the edge of the hole. The second path was created from the bottom edge to the edge of the hole whereas the third path was created along the edge of the hole from its left-most point to its bottom-most point. These total 12 paths were used to create 12 plots for von Mises stresses in the plate by using the XY Data. The data generated was exported to Excel to create plots.

III. RESULTS

A. Analytical Results

The analytical solution for the von Mises stresses in the uniaxially loaded plate with a hole can be calculated by finding out the cylindrical plane stress components. To calculate these stress components, Kirsch's Solution was utilised.

$$\sigma_r = \frac{\sigma}{2}\left(1-\left(\frac{a}{r}\right)^2\right)+\frac{\sigma}{2}\left(1-4\left(\frac{a}{r}\right)^2+3\left(\frac{a}{r}\right)^4\right)cos\,2\theta \quad (7)$$

$$\sigma_\theta = \frac{\sigma}{2}\left(1+\left(\frac{a}{r}\right)^2\right)-\frac{\sigma}{2}\left(1+3\left(\frac{a}{r}\right)^4\right)cos\,2\theta \quad (8)$$

$$\tau_{r\theta} = -\frac{\sigma}{2}\left(1+2\left(\frac{a}{r}\right)^2-3\left(\frac{a}{r}\right)^4\right)sin\,2\theta \quad (9)$$

where a= radius of the hole (mm)
r= radial distance from the centre of the hole (mm)
θ= angle from the direction of the load (radians)
σ_r= normal stress along radial direction (MPa)
σ_θ= normal stress along the angular direction (MPa)
$\tau_{r\theta}$= shear stress (MPa)

After obtaining the plane stress components, the von Mises stresses were calculated using the cylindrical form of Eq. (5):

$$\sigma_v = \sqrt{\sigma_r{}^2 + \sigma_\theta{}^2 - \sigma_r\sigma_\theta + 3\tau_{r\theta}{}^2} \qquad (10)$$

MATLAB software was used to develop a function to calculate the von Mises stress using Eq. (10). The function was used in a code to generate the values along the same edges that were used to create paths in Abaqus. The following plots were obtained for von Mises stresses along the horizontal and vertical axes of symmetry, and along the edge of the hole. The maximum stress was found to occur on the left-most edge of the hole with a magnitude of 150 MPa.

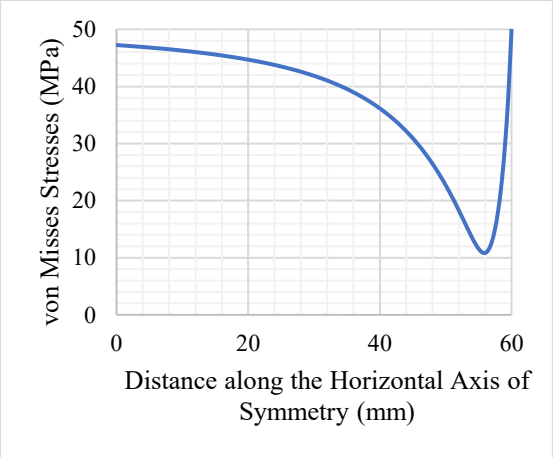

Fig.1. Analytical von Mises Stress Results along the Horizontal Axis of Symmetry

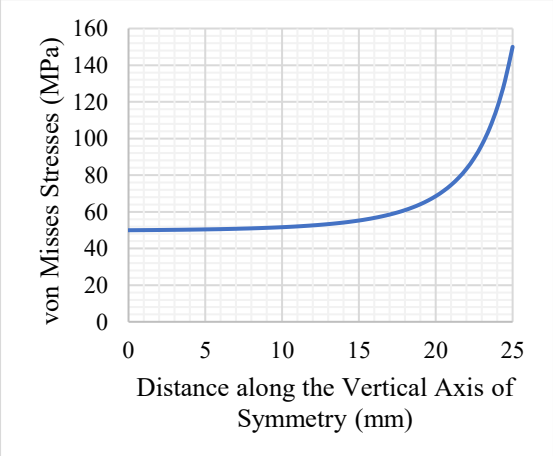

Fig.2. Analytical von Mises Stress Results along the Vertical Axis of Symmetry

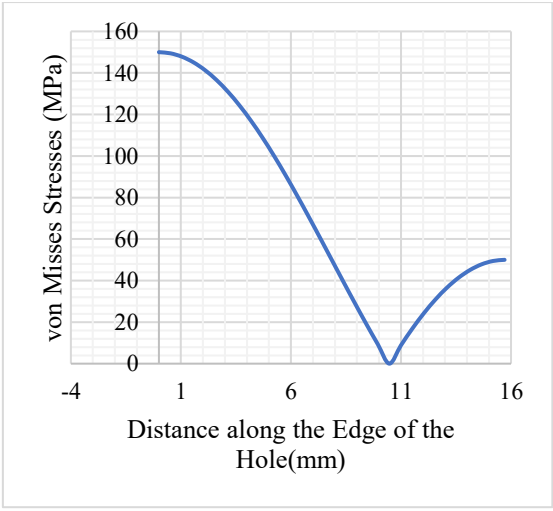

Fig.3. Analytical von Mises Stress Results along the Edge of the Hole

B. Numerical Results

1. Full Plate

The full plate model subjected to uniaxial tensile load presented the following deformed shape. The colour contours show that the maximum von Mises stress is along the top and bottom edge of the hole with a magnitude of 150.5 MPa. Similar stress concentration behaviour under uniaxial tensile loading in plates with central circular holes has been numerically demonstrated using FEA [14-15].

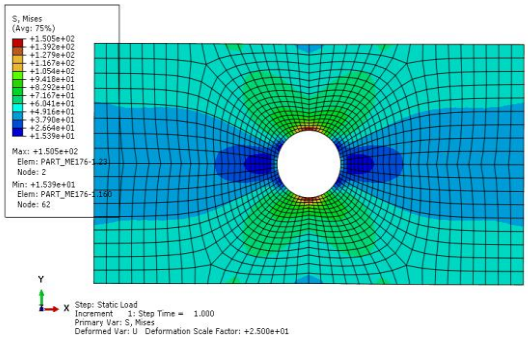

Fig.4. Deformed Shape of the Full Plate Model

2. Left Half Plate

The left half plate model subjected to uniaxial tensile load on the left edge and symmetry boundary condition on the right presented the following deformed shape. The colour contours show that the maximum von Mises stress is along the top and bottom edge of the notch having a magnitude of 148.3 MPa.

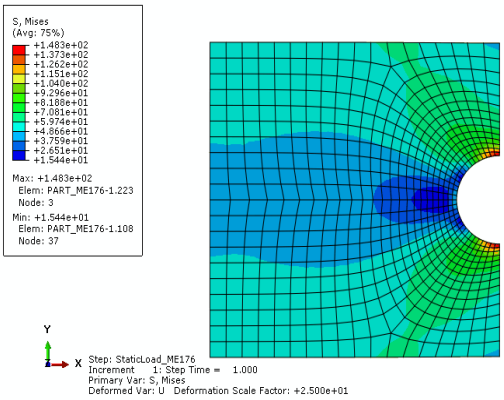

Fig.5. Deformed Shape of Left Half Plate Model

3. *Lower Half Plate*

The lower half plate model subjected to uniaxial tensile load on both sides edge and symmetry boundary condition on the top edge presented the following deformed shape. The colour contours show that the maximum von Mises stress is along the bottom edge of the notch having a magnitude of 150.4 MPa.

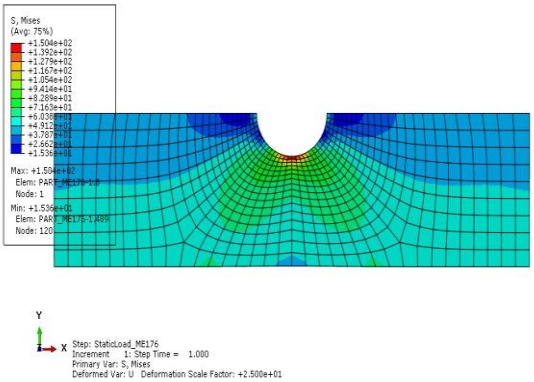

Fig.6. Deformed Shape of Lower Half Plate Model

4. *Quarter Plate*

The quarter half plate model subjected to uniaxial tensile load on the left edge and symmetry boundary condition on the right presented the following deformed shape. The colour contours show that the maximum von Mises stress is along the bottom edge of the arc with a magnitude of 148.2 MPa.

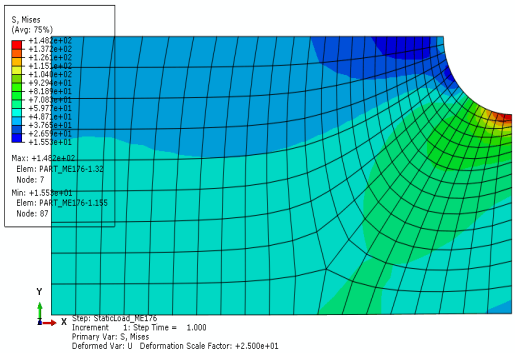

Fig.7. Deformed Shape of Quarter Plate Model

IV. Discussion

C. *Along Horizontal Axis of Symmetry*

The following plot of the von Mises stress along the horizontal axis of symmetry was obtained by using all the numerical data along with the analytical results. It can be seen that all numerical results are in perfect agreement with each other. They almost perfectly overlap each other. However, the analytical results seem to stay a little lower than the numerical results along the entire path with the greatest difference among them occurring at about 56mm from the outer edge along the horizontal axis of symmetry. The average stress shown by all the numerical results at this point is about 15.44 MPa while the analytical results provide a value of 10.85 MPa. The total error in this case comes out to be 42.33%.

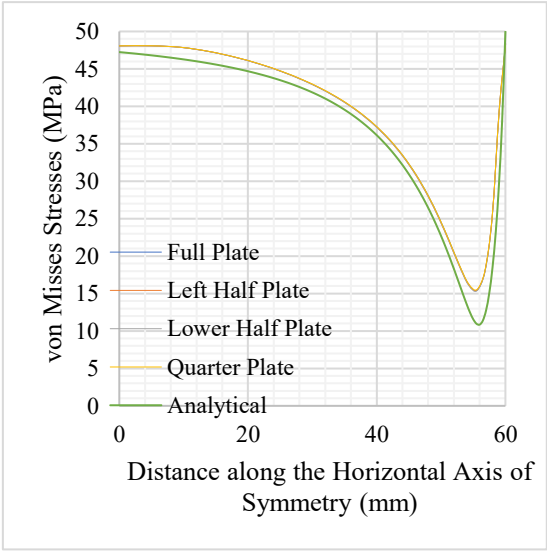

Fig.8. Comparison of the von Mises Stress obtained along the Horizontal Axis of Symmetry with Numerical and Analytical Methods

D. *Along the Vertical Axis of Symmetry*

The following plot of the von Mises stress along the vertical axis of symmetry was obtained by using all the numerical data along with the analytical results. It can be seen that all numerical results are in perfect agreement with each other. They almost perfectly overlap each other. The only exception being the lower half plate which deviates from the rest at the end by a difference of about 2 MPa. The analytical results show higher stress at the edge. The error between the analytical results and the average numerical results at this point is about 5%. As we move along the edge, Fig. (9) replicates the pattern of Fig. (8) with analytical results staying a little lower than the numerical results. At the end of the edge an interesting point can be observed. The numerical results of full plate and lower half plate seem to converge better than the others with the analytical results. The percentage error of both the

lower half plate and the full plate at this point is about 0.3% while the error of the other two models comes out to be around 1%.

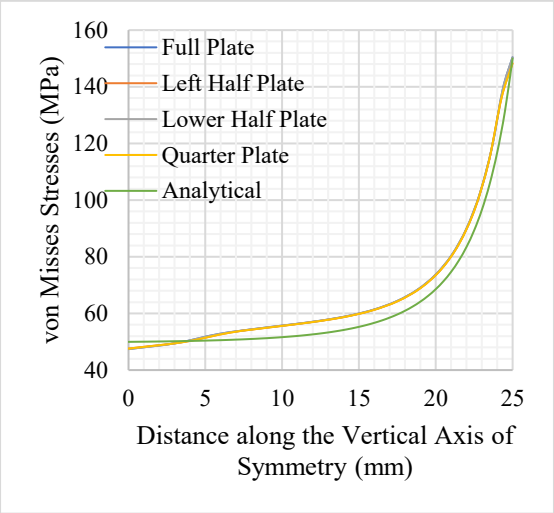

Fig.9. Comparison of the von Mises Stress obtained along the Vertical Axis of Symmetry with Numerical and Analytical Methods

E. Along the Edge of the Hole

The following plot of the von Mises stress along the edge of the hole of the plate was obtained by using all the numerical data along with the analytical results. It can be seen that all numerical results are in good agreement with each other at most of the points. At the start, which is the bottom-most edge of the hole, the lower half plate and the full plate seem to be in better agreement with the analytical results than the other two models [16]. Experimental studies on strain and stress concentrations in composite laminates with central holes show similar agreement trends between numerical and physical results [17]. It must be noted here that this is the same point where Fig. (9) ended. Previously discussed figures mostly showed numerically calculated stresses to be greater than analytically calculated ones but along the edge a different story can be seen [18], where the numerical results are lesser than the analytical results for half the distance along the edge (about one-eighth of the circumference around the hole). A significant dip is seen in the analytically calculated stresses as they effectively drop to zero around 10.5 mm from the bottom-most point along the curved edge. The difference between the average of all numerical results and the analytical value at this point is 19.23 MPa [19]. If the percentage error was calculated at this point, it would come out to be infinity.

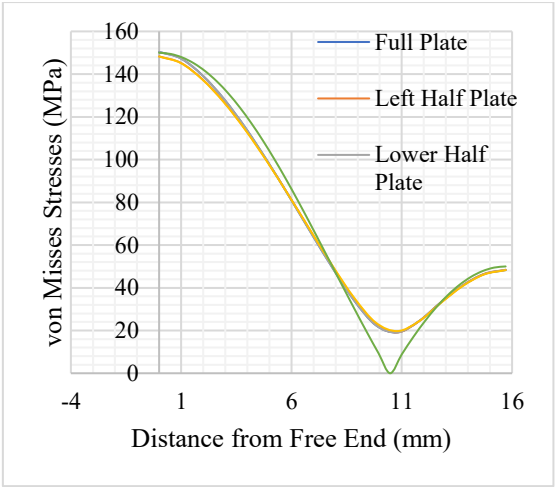

Fig.10. Comparison of the von Mises Stress obtained along the Edge of the Hole with Numerical and Analytical Methods

F. Mesh Sizing

Although finer mesh was used near the stress concentration regions, it still failed to capture some extreme cases of stress deprivation [20]. To get better results around the hole, an even finer mesh must be used. However, this might compromise the primary objective of saving computational time.

V. Conclusion

- All simplified models (left half, lower half, and quarter) showed von Mises stress distributions that closely matched the full plate model along the horizontal and vertical axes of symmetry.
- Minor deviations (within 5%) occurred near the stress concentration regions, particularly along the curved edge of the hole.
- The lower half and full plate models performed slightly better at capturing local dips near the hole edge
- Among all models, the quarter plate provided the most efficient balance between computational cost and accuracy
- The study confirms that symmetry-based reductions can be confidently used in FEM of symmetry geometries without significant loss of accuracy

References

[1] M. Asgari and M. A. Kouchakzadeh, “An improved plane strain/plane stress peridynamic formulation of the elastic–plastic constitutive law for von Mises materials,” *Engineering with Computers*, vol. 40, no. 4, pp. 2127–2142, 2024, doi: https://doi.org/10.1007/s00366-023-01898-5.

[2] R. H. Patel and B. P. Patel, "Analyzing stress concentration factor in finite plate with different polygonal discontinuities under uniaxial compression using FEM," *Jurnal Kejuruteraan*, vol. 35, no. 5, pp. 1033–1043, 2023, doi: https://doi.org/10.17576/jkukm-2023-35(5)-05.

[3] M. S. Islam, "Finite Element Approach to Analyze Structural Discontinuities Associated with Ship Hull," 2023, doi: https://dx.doi.org/10.2139/ssrn.4447483.

[4] R. H. Patel and B. P. Patel, "Effect of various discontinuities present in a plate on stress concentration: a review," *Engineering Research Express*, vol. 4, no. 3, p. 032001, 2022, doi: https://doi.org/10.1088/2631-8695/ac8c1b.

[5] R. Chugh, S. Nagpal, and S. Sanyal, "Parameters for Mitigation of Stress Concentration Factor in a Thin Curved Plate with Single Circular Hole Under Tensile Load," *Journal of Failure Analysis and Prevention*, pp. 1–16, 2025, doi: https://doi.org/10.1007/s11668-025-02132-8.

[6] B. P. Patel and R. H. Patel, "Determination and analysis of stress concentration factor in finite plate with different polygonal discontinuities under uniaxial compression using finite element analysis (FEA)," *Engineering Research Express*, vol. 6, no. 2, p. 025552, 2024, doi: https://doi.org/10.1088/2631-8695/ad51ce.

[7] T. da Silveira, C. Fragassa, L. A. O. Rocha, E. D. dos Santos, and L. A. Isoldi, "Geometric Investigation of Thin Perforated Steel Plates Under Biaxial Elasto-Plastic Buckling by using Constructal Design," *Reports in Mechanical Engineering*, vol. 5, no. 1, pp. 43–67, 2024, doi: https://doi.org/10.31181/.

[8] R. H. Patel and B. P. Patel, "Experimental And Numerical Investigation of Stress Concentration Factor for Polygonal Discontinuities In A Finite Plate," *Reliability: Theory & Applications*, vol. 19, no. 4 (80), pp. 325–342, 2024.

[9] M. Sivaramakrishnaiah, S. N. P. Reddy, P. M. Raghava, and B. V. Amaranathareddy, "Theoretical and simulation of central elliptical hole with rectangular plate," *Journal of Emerging Science and Engineering*, vol. 2, no. 1, p. e18, 2024, doi: https://doi.org/10.61435/jese.2024.e18.

[10] A. A. Hamed, A. Samadi, and M. C. Basim, "Topology and shape optimization of steel plate shear walls for enhancing the seismic energy dissipation capacity," *Journal of Building Engineering*, vol. 57, p. 104828, 2022, doi: https://doi.org/10.1016/j.jobe.2022.104828.

[11] V. Hassani, H. A. Mehrabi, Z. Ibrahim, and I. F. Ituarte, "A Comparison between Parametric Structural Optimization Methods and Software-Based Topology Optimization of A Rectangular Sample Under Tensile Load for Additive Manufacturing Processes," *International Journal of Engineering Research and Applications*, vol. 11, no. 2, pp. 37–58, 2021, doi: https://doi.org/10.9790/9622-1102063758.

[12] M. Fuentetaja-Merino, A. Silva-Campillo, M. A. Herreros-Sierra, and F. Pérez-Arribas, "Structural Analysis of the Geometric Alternatives of Double-Bottom Floor Plates of a Panamax-Class Container Ship," *Applied Sciences*, vol. 14, no. 22, p. 10684, 2024, doi: https://doi.org/10.3390/app142210684.

[13] M. Li, E. Oterkus, and S. Oterkus, "A two-dimensional four-node quadrilateral inverse element for shape sensing and structural health monitoring," *Mathematics and Mechanics of Solids*, vol. 29, no. 7, pp. 1364–1378, 2024, doi: https://doi.org/10.1177/10812865231224438.

[14] D. Castagnetti and E. Dragoni, "Stress distributions around the interference fit between a round pin and a perforated finite plate," *Journal of the Brazilian Society of Mechanical Sciences and Engineering*, vol. 46, no. 4, p. 219, 2024, doi: https://doi.org/10.1007/s40430-024-04811-3.

[15] A. Kacimi, G. Ikhenazen, F. Mohri, M. Saidani, and M. Kilardj, "Linear and nonlinear stability analysis of thin rectangular plates subjected to local in-plane shearing," *Structural Engineering International*, vol. 33, no. 4, pp. 689–698, 2023, doi: https://doi.org/10.1080/10168664.2023.2208143.

[16] K. Hazizi, M. Ghaleeh, and S. Rasool, "Analytical and Numerical Investigation of Fatigue Life in Rectangular Plates with Opposite Semicircular Edge Single Notches," *Applied Mechanics*, vol. 4, no. 3, pp. 948–973, 2023, doi: https://doi.org/10.3390/applmech4030049.

[17] T. S. Dawood and Y. K. Khdir, "Effect of Crack Length on Stresses in a Plate with a Hole," *Al-Nahrain Journal for Engineering Sciences*, vol. 25, no. 1, pp. 28–34, 2022, doi: http://doi.org/10.29194/NJES.25010028.

[18] M. Noori, A. Bilgin, H. Diallo, M. O. Al Rousan, and A. R. Noorı, "A study on the influence of material gradient index on bending and stress responses of FGM rectangular plates using the Finite Element Method," *Journal of Sustainable*

Construction Materials and Technologies, vol. 9, no. 3, pp. 239–254, 2024, doi: https://doi.org/10.47481/jscmt.1555157.

[19] M.-H. Safari-Naderi, M. Shakouri, and A. Ghasemi-Ghalebahman, "A bond-based peridynamics model based on variable material properties for modeling elastoplastic behavior," *Materials Today Communications*, vol. 35, p. 105890, 2023, doi: https://doi.org/10.1016/j.mtcomm.2023.105890.

[20] S. Ch. Djebbar, K. Madani, M. El Ajrami, A. Houari, N. Kaddouri, M. Mokhtari, X. Feaugas, and R. D. S. G. Campilho, "Substrate geometry effect on the strength of repaired plates: Combined XFEM and CZM approach," *International Journal of Adhesion and Adhesives*, vol. 119, p. 103252, 2022, doi: https://doi.org/10.1016/j.ijadhadh.2022.103252.